Vacuum 215 (2023) 112283

Contents lists available at ScienceDirect

Vacuum

journal homepage: www.elsevier.com/locate/vacuum

Graphene oxide modifications by X-rays irradiations in air and vacuum

L. Torrisi [a,b,*], M. Cutroneo [c], A. Torrisi [d,**], L. Silipigni [a,b]

[a] Department of Mathematics and Computer Sciences, Physical Sciences and Earth Sciences (MIFT), University of Messina, V.le F.S. d'Alcontres 31, 98166, Messina, Italy
[b] Istituto Nazionale di Fisica Nucleare, Sezione di Catania, Via S. Sofia 62, 95123, Catania, Italy
[c] Nuclear Physics Institute of the CAS, Hlavní 130, 250 68, Husinec Řež, Czech Republic
[d] Interuniversity Department of Physics, University of Bari, 70126, Bari, Italy

ARTICLE INFO

Handling Editor: Prof. L.G. Hultman

Keywords:
Graphene oxide
Reduction
Oxidation
X-rays irradiation
FTIR spectroscopy

ABSTRACT

Graphene oxide (GO) foils have been exposed to X-rays in air and in vacuum. The attenuated total reflectance (ATR) method for Fourier Transmission Infrared (FTIR) spectroscopy has been used to analyze the pristine and the irradiated GO foils. The X-ray exposition in air produces oxidation increment, while in vacuum it induces reduction of the oxygen functional groups and partial removal of water. These processes have been investigated as a function of both the irradiation time and X-ray energy distribution highlighting the variations of some functional groups of oxygen. Some interesting applications of the GO reduction will be suggested in the field of ionization dosimetry, detectors, microelectronic devices, and membranes, as presented hereafter.

1. Introduction

Graphene represents a two-dimensional carbon allotropic state and consists in a single layer of carbon atoms arranged in a honeycomb-like nanostructure where each carbon atom is connected to its three nearest neighbors by a strong σ-bond [1].

Graphene oxide (GO) represents the oxidized form of graphene: it consists of one or a few layers of carbon atoms with oxygen functional groups attached to both sides of the carbon layers and at the edges. It is easy to process since it is dispersible in water and other solvents and its quality and applications depend on both the number of carbon atoms layers and the carbon/oxygen ratio value. The electrical insulating nature of GO is attributable to the oxygen presence in its structure. It can be reduced to graphene by different processes [2]. Generally, GO is obtainable as thin film or thick foil depositing, by the spin coating technique, the suspension obtained after the graphite chemical exfoliation by the Hummer's method [3], on appropriate substrates, and letting it dry in air. The deposited suspension can contain layers, monolayers, and sometimes micrometric sheets of GO [4,5].

Graphene oxide (GO) is an exceptional material with unique properties [6], suitable for detecting ionizing radiations [7] and making membranes [8], highly responsive to temperature variation and treatments [9] like lamp and laser irradiations [10]. It has been successfully employed as flexible substrate for microelectronic devices [11], to realize different sensors [12], diodes and transistors [13], and for many other applications.

GO contains oxygen functional groups, such as hydroxyl (-OH), carbonyl (C═O), carboxyl (O═C–OH) and epoxydic (-C-*O*-C), water and other gases (H_2, N_2, CO_2, …), as evinced by X-ray photoelectron spectroscopy (XPS) [14,15]. It behaves like a sponge that absorbs water and gas, storing them in large quantities. The quantity of oxygen functional groups and water can be increased by oxidative processes, such as thermal processes in air or reactive gases, which make the material absorbent in the visible and IR range, electrically insulating, extremely light and hydrophilic [2].

The reduction of the functional groups can be obtained in vacuum or inert environment, with thermal treatments, exposition to different ionizing radiations, UV lamps [16], lasers and chemically [17,18] in the attempt of obtaining the graphene properties.

Literature reports that the GO exposition to IR laser pulses in air and in vacuum produces different effects, of oxidation in the former case and reduction in the latter one [19].

The reduced graphene oxide (rGO) can have different levels of reduction depending on the quantity of oxygen functional groups

* Corresponding author. Department of Mathematics and Computer Sciences, Physical Sciences and Earth Sciences (MIFT), University of Messina, V.le F.S. d'Alcontres 31, 98166, Messina, Italy.
** Corresponding author.
E-mail addresses: lorenzo.torrisi@unime.it (L. Torrisi), alfio.torrisi@uniba.it (A. Torrisi).

https://doi.org/10.1016/j.vacuum.2023.112283
Received 4 April 2023; Received in revised form 14 May 2023; Accepted 10 June 2023
Available online 10 June 2023

remaining in the structure. However, even low concentrations of oxygen functional group make rGO very different from graphene. For instance, GO modified into reduced GO (rGO) becomes electrically and thermally conductive, very transparent to IR radiation, it assumes greater density, from about 1.36 g/cm^3 up to about 1.9 g/cm^3, and hydrophobic characteristics [20].

Due to the different processes of oxidation or reduction in GO, producing a material with different physical and chemistry characteristics, it is possible to realize different devices and sensors operating at the macroscopic and microscopic scales. In fact, it is possible to realize conductive tracks of rGO with micrometric thickness on the insulating GO substrates [21] for the manufacturing of electric resistances, micro capacitors, FET transistors, and microcircuits on such mechanically resistant and perfectly flexible substrates [10].

The GO research activity is also finding interesting applications in the field of dosimetry of ionizing radiations since the level of GO reduction increases proportionally at the absorbed dose, as reported in the literature [22]. Moreover, other important applications are based on the GO properties and its modification in rGO, such the gas diffusion through GO and rGO membranes controlled by the level of reduction [23], the contact potential in metal-GO junctions to realize batteries and diodes [24,25]. Also, ion strippers for ion accelerator sources, based on GO and rGO thin films, can be used with advantage with respect to the traditional graphite strippers [26]. The high content of hydrogen in GO, its crystalline structure and low density can be employed to obtain highly energetic proton bunches at high current by using laser-generated plasma in the target-normal-sheath-acceleration (TNSA) regime [27]. These are only a few of the more prominent applications that currently are under investigation to obtain innovative materials, devices and sensors useful in different scientific fields, from Biology and Medicine to Microelectronics and Chemistry, and from Physics and Engineering to environment and cultural heritage.

The GO oxidation or reduction, doping, interlamellar conduction of atomic and molecular species, luminescence and other properties of composite materials based on GO and rGO are becoming of high interest for the innovative technologies. Just think of the new lithium graphene oxide batteries [28], the new electronics on flexible GO sheets [29], the use of *n* and *p* doped rGO [30] and the realization of innovative small GO dosimeters for ionizing radiations [31].

In our previous papers we studied the effects produced in GO by non-monochromatic X-rays at 1.5 keV in vacuum [32] and by IR laser irradiation in air and vacuum [19]. The irradiated materials have been analyzed using XPS, electron microscopy and associated energy dispersive X-Ray (EDX) Analysis. The X-ray and IR laser irradiations in vacuum reduce the oxygen content in GO, while the GO IR laser irradiation in air increases the oxygen content at fluences lower than 400 mJ/cm^2 and reduce it at higher fluences. In this work, we wanted to investigate how the response of the GO to non-monochromatic X-ray radiation, up to a maximum energy of about 30 keV, in air and in vacuum changes as a function of the bias voltage applied to the X-ray tube and the exposure time. To obtain this information we have not used XPS and SEM/EDX analysis, which properties applied to GO and rGO were already presented in our previous papers [7,32], but we have used the simplest, but no less accurate, attenuated total reflectance coupled to Fourier transform infrared (ATR-FTIR) spectroscopy.

2. Experimental set-up

GO foils have been purchased from Graphenea [33] in the form of discs with a diameter of 4 cm and a uniform thickness of 15 μm. The Graphenea GO composition is: Carbon = 49–56%; Hydrogen = 0–1%; Nitrogen = 0–1%; Sulphur = 2–4%; Oxygen = 41–50%.

The color of the GO foil is black and its electrical conductivity at room temperature very low, of about 10^{-10} Ω^{-1}cm^{-1}.

The X-rays source consists of a compact miniaturized X-ray tube system produced by the AMETEK, USA [34]. The system, called Mini-X2 tube, also includes the power supply, the control electronics and the USB communication to the computer. It is optimized for portable characteristics X-ray fluorescence (XRF) analysis. It has a maximum power of 10 W and works with a controllable power supply whose maximum value is 50 kV and maximum current 200 μA. The X-ray source anode is Ag, but it can be replaced with Au, Rh, or W anodes. The remote control permits to select the tube voltage between 10 and 50 kV and the current from 10 to 200 μA. The tube has a final aluminum/brass collimator with 2 mm diameter hole. AMETEK system gives an output dose rate of about 1 Sv/h at 30 cm on axis, at a 50 kV voltage and with the Ag anode.

Fig. 1 shows a photo of the flexible GO foil (a) and of the X-ray tube (b) used in this investigation. The X-ray tube emission spectrum, as given by AMETEK using a semiconductor detector, is constituted by a Compton background and by the overlapped characteristic lines, $L_{\alpha,\beta,\gamma}$ (2.98 keV, 3.3 keV, 3.5 keV) and $K_{\alpha,\beta}$ (22.2 keV, 24.9 keV) of the used Ag anode.

Fig. 2a shows typical emission spectra of the Mini-X2 X-ray tube using the Ag anode at different bias voltages between 10 kV and 50 kV. The Ag X-ray K-peaks are displayed only if the working voltage of the tube is higher that the ionizing potential of the Ag K-shell which is of about 22.2 keV. By considering the peak of the Bremmstrahlung distribution given by AMETEK (Fig. 2a), the mean X-ray energy is about 9 keV, 12 keV and 13–14 keV in the case of use of 10 kV, 20 kV and 30 kV tube bias voltages, respectively.

The picture of the adopted system illustrating the vacuum chamber in which the GO foil has been irradiated, in both the two configurations of air and vacuum (10^{-3} mbar), is displayed in Fig. 2b. It is a system for X-ray fluorescence (XRF) spectroscopy also containing the Si-PIN detector and its relative detection electronics, which is connected to a multichannel analyzer for elemental analysis. The GO X-ray irradiation in vacuum, at 19 cm from the X-ray tube collimator output, has been performed with different tube voltages (10 ÷ 30 kV) and exposition times (30, 60 and 120 min). Instead, the GO irradiation with X-ray in air was first performed at 19 cm in the same chamber without evacuating it at the same exposure times. Since the observed changes were less evident, the GO irradiation with X-ray in air was then carried out at 3 cm at the same tube voltages and exposure times used for the vacuum X-ray irradiation.

The ATR-FTIR spectroscopy has been employed to analyze the pristine GO foils and the irradiated ones, which have been reduced at a size of about 1 cm^2 each. The used instrument was a Jasco ATR-FTIR spectrometer, Mod. 4600, operating at a 4 cm^{-1} resolution in the (400–4000) cm^{-1} wavenumber range [35].

3. Results and discussion

The pristine GO foil analyzed by ATR-FTIR spectroscopy shows the typical transmission peaks due to the different oxygen functional groups, as visible in the spectrum of Fig. 3 in which the IR transmittance is plotted vs. the wavenumbers.

In fact the spectrum, acquired in air, reveals the GO characteristic IR absorption peaks at 1728, 1628, 1422 and 1052 cm^{-1}, which can be attributed to the stretching vibrations of C═O in the carboxyl and carbonyl groups, partly of C═C from the unoxidized graphitic domain partly of C═O from the carbonyl groups, of C–O in the carboxylic groups and in the epoxide bonds respectively. The strong broad band centered at approximately 3200 cm^{-1} can be assigned to the O–H stretching modes of the hydroxyl groups present in the absorbed water molecules or in the phenolic or carboxylic groups. The obtained spectrum is in good agreement with the similar investigation of GO foils reported in the literature [36].

Fig. 4a shows the comparison of the ATR-FTIR spectra relative to the GO foils pristine and X-ray irradiated in air at room temperature (about 22 °C), with 50% air humidity and at a 1 bar pressure; the X-ray tube operated at the 10 kV bias voltage, at a 3 cm collimator-sample distance and for 30, 60, and 120 min (min) exposition times. The ATR-FTIR

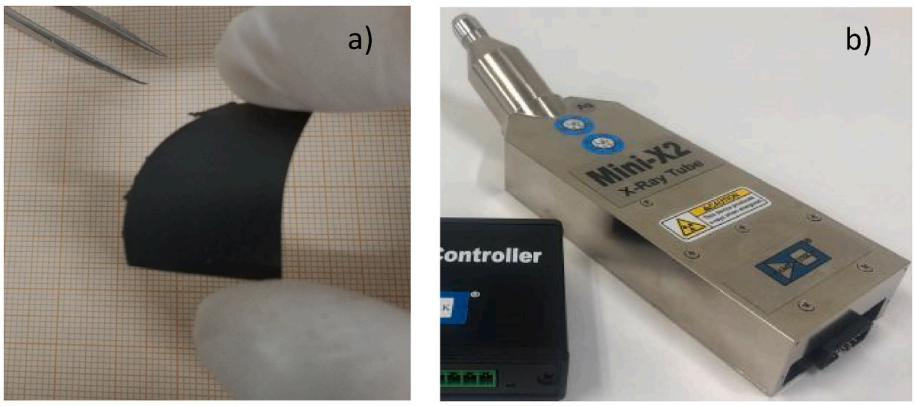

Fig. 1. The GO foil (a) and the Mini-X2 X-ray tube (b).

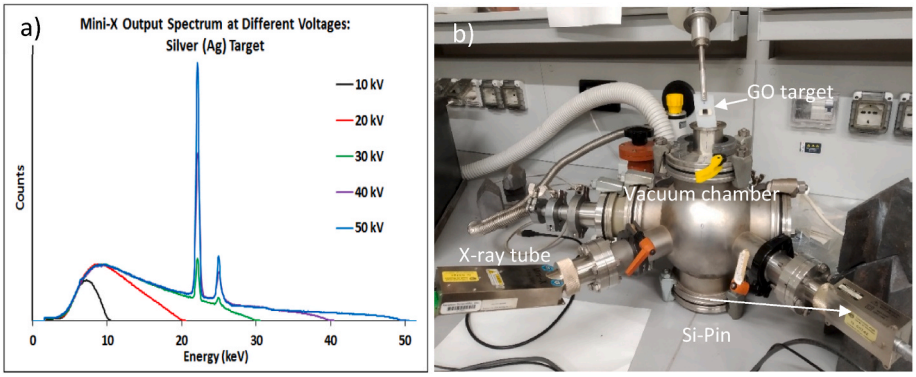

Fig. 2. Mini-X2 silver emission spectra at voltages within 10–50 kV (a) and a photo of the experimental set-up for the GO irradiation.

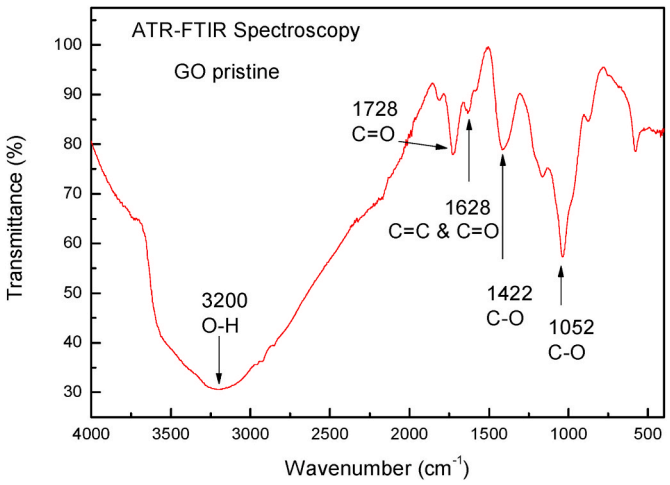

Fig. 3. ATR-FTIR spectrum of the pristine GO foil.

spectra comparison indicates that the GO irradiation in air causes a further significant oxidation of the treated samples. In facts, the in-air X-ray exposition produces chemical bonds breaking and formation of reactive radicals, with generation of more C–O bonds and further GO oxidation, as observable from the intensity variations of the transmission peaks. In particular, the main vibrational bands due to OH (3200 cm^{-1}), C═O (1728 cm^{-1}), and C–O (1422 and 1052 cm^{-1}) enhance, due to their concentration increment. This phenomenon decreases the IR transmission in the (400–4000) cm^{-1} wavenumber range.

As already said in the experimental section, the GO X-ray irradiation was also performed within the vacuum chamber without evacuating it at 19 cm distance from the X-tube collimator, a distance due to the vacuum chamber geometry and X-ray tube assembly. In this case, as one can see in Fig. 4b, the oxidation process in air is less evident because the X-ray intensity decreases with the square of the distance and less dose is absorbed by the irradiated GO at the same exposition times giving a minor oxidation.

Fig. 5 shows a similar ATR-FTIR spectra comparison to that of Fig. 4a with the only difference being that the X-ray tube operated at a bias voltage of 30 kV. It is possible to evaluate an effect of oxidation which is comparable to that obtained in the 10 kV bias voltage case. However, at this X-ray energy, it is possible to also observe the appearance of structures around 2355 cm^{-1}, which become increasingly evident as the irradiation time increases. These features, already slightly visible at 10 kV, are due to the formation of CO_2 molecules in agreement with the literature [37]. The intensity of these features is proportional to the X-ray exposition time increasing with the level of reduction, as will be better described in the following.

A different process occurs in vacuum with respect to the air irradiation. Also, in vacuum the X-ray exposition produces chemical bonds breaking and formation of reactive radicals, but the absence of air and the free molecules diffusion toward the pumping system driven by the pressure gradient reduce the oxygen functional groups and water in the irradiated GO, i.e., the in vacuum X-ray exposition induces a significant GO reduction effect which has been observed by the ATR-FTIR spectroscopy.

Fig. 6 displays the comparison of the results obtained for GO irradiated in vacuum (10^{-3} mbar), at room temperature (22 °C), at the 10 kV bias voltage, at a 19 cm collimator-sample distance, and for 30, 60, and 120 min exposition times. In this case the vibrational bands due to OH (3200 cm^{-1}), C═O from the carbonyl groups (1628 cm^{-1}) and C–O from carboxylic and epoxide groups (1422 and 1052) are reduced in

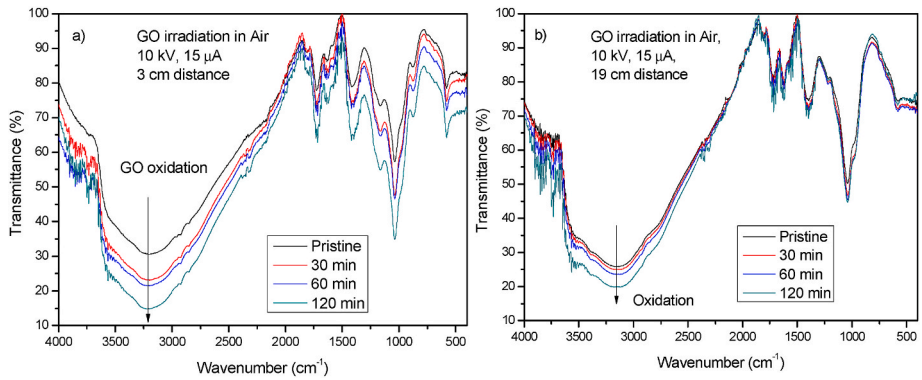

Fig. 4. Comparison between the ATR-FTIR spectra of GO pristine and GO X-ray irradiated in air at the 10 kV bias tube voltage for 30, 60 and 120 min at 3 cm (a) and 19 cm (b) from the X-ray tube collimator: the X-ray irradiation induces oxidation processes in GO.

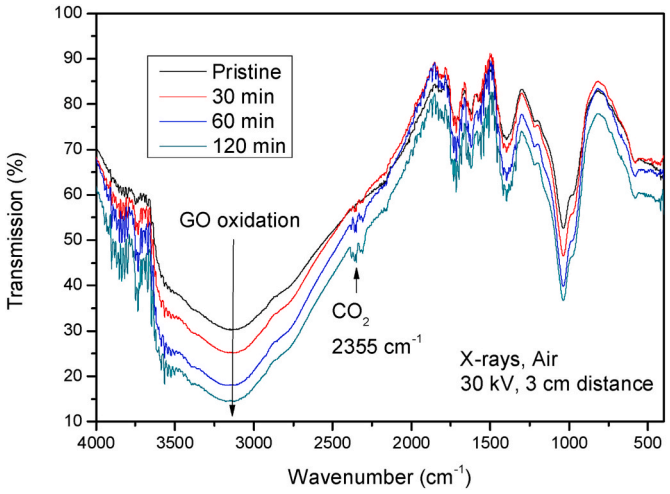

Fig. 5. Comparison between the ATR-FTIR spectra of GO pristine and GO X-ray irradiated in air at the 30 kV bias for 30, 60 and 120 min: the X-ray irradiation induces oxidation processes in GO.

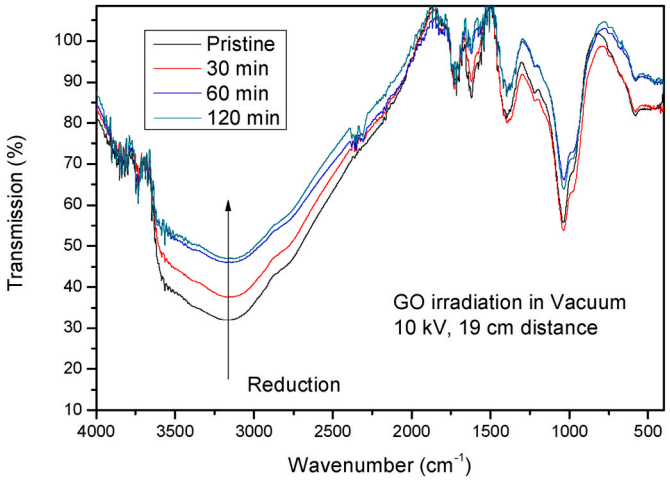

Fig. 6. Comparison between the ATR-FTIR spectra of GO pristine and GO X-ray irradiated in vacuum at the 10 kV bias for 30, 60 and 120 min: the X-ray irradiation induces reduction processes in GO.

intensity, i.e., enhanced in transmission, due to their minor concentration in the GO and less IR absorption. Thus, the material results less rich in oxygen functional groups and water and more transparent to the IR radiation demonstrating that the X-rays induce a GO reduction degree proportional to their exposition time. The reduction effect can be quantized by the large and intense O–H vibrational band whose transmission, with respect to the pristine sample, increases of about 19.4% at a 30 min exposition time up to about 51.6% at a 120 min exposition time. It is possible to observe a saturation trend at exposition times higher than 60 min.

The use of more energetic X-rays, i.e., more penetrating, obtainable increasing the mini tube bias voltage, should change the reduction effect in vacuum, as expected for the minor absorption in the thin GO foil. Based on this consideration, measurements have been conducted using the 15 kV and 30 kV bias voltages with the same current and exposition times of 30, 60 and 120 min in vacuum at room temperature. Fig. 7 report an ATR-FTIR spectra comparison between the pristine GO and rGO obtained for different irradiation times using the 15 kV (a) and 30 kV (b) bias voltages in vacuum.

As one can see by comparing Fig. 6 and Fig. 7 the GO reduction effect seems to increase with the X-ray bias voltage in vacuum, probably due to the vacuum assisted removing of the molecules detached from GO or desorbed from the carbon sheets surface. It should be noted that the ATR-FTIR spectra of the GO pristine foils shown in Figs. 3–7 present slight variations in the IR transmittance values. This occurs because, to realize the different investigated X-ray exposure sets, various GO pristine foils, which evidently slightly differ in local composition and therefore in the oxygen content, were used. This does not invalidate the presented measurements and their discussion because the state of GO oxidation or reduction is evaluated with reference to the IR transmittance value of the relative GO pristine sample irradiated by X-rays. Furthermore, our attention is focalized on the IR transmittance trend and not on its absolute values.

For instance, the O–H transmission IR band at 3200 cm^{-1} shows a transmittance variation with the X-ray irradiation time demonstrating the different effects of oxidation in air (transmittance reduction and absorbance increment of the O–H groups) and reduction in vacuum (transmittance increment and absorbance decrease of the OH-groups), as reported in Fig. 8.

An investigation like this can be also done for other main peaks detected by FTIR spectroscopy. For instance, two important peaks are those due to the C–O epoxide group at 1052 cm^{-1} and to the C═C bonds & C═O carbonyl group at 1628 cm^{-1}. Although it is clear from our measurements that such peaks decrease in transmittance during the oxidation process and increase in transmittance during the reduction process, their transmittance evaluation as a function of the irradiation time is not so simple because it depends on the background value which has some little oscillations as evident from the above presented spectra. Such oscillations are imputable to two desorption mechanisms: 1) the emission of oxygen functional groups which occurs not only from the GO surface but also from the inner GO layers and 2) the release not only of

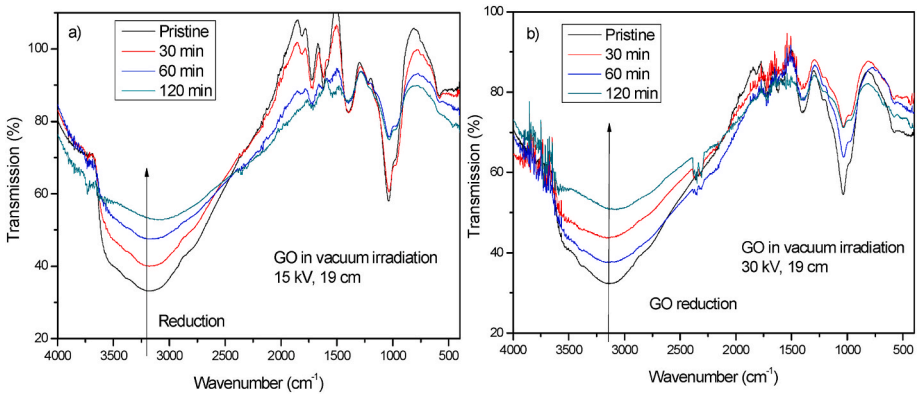

Fig. 7. Comparison between the ATR-FTIR spectra of GO pristine and GO irradiated at the 15 kV (a) and 30 kV (b) bias voltages in vacuum for 30, 60 and 120 min. In this case the X-ray exposure induces reduction processes.

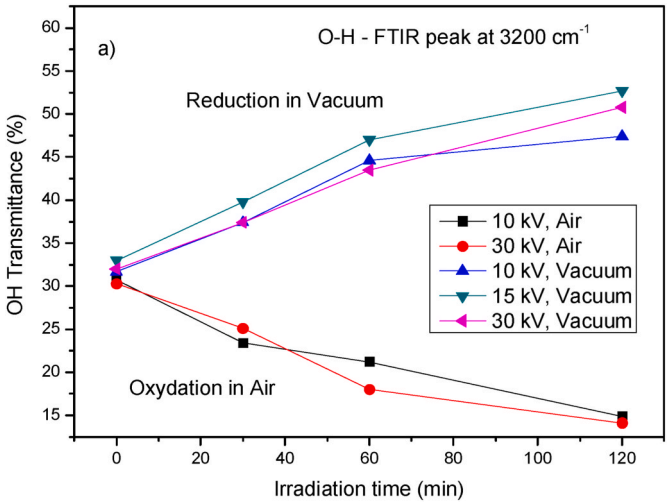

Fig. 8. O–H stretching IR band transmittance versus the X-ray irradiation time in air and in vacuum at different bias voltages of the X-ray mini tube.

single molecules but also of molecules aggregates in air and in vacuum.

The C–O and C═C & C═O peaks transmittance, observed at 1052 cm^{-1} and 1628 cm^{-1}, respectively, is plotted versus X-ray irradiation time, as shown in Fig. 9a and b, respectively. Despite the fluctuations of IR transmittance signal, the C–O peak shows a transmittance which decreases with the oxidation process both at 10 kV and at 30 kV in air, proportionally to the X-ray irradiation time. In vacuum this transmittance increases, as result of a significant GO reduction due to the decrement of C–O molecular bonds, as shown in the plot of Fig. 9a.

With respect to the C═C & C═O peak at 1628 cm^{-1} its transmittance also results significantly influenced by the X-ray irradiation in air and in vacuum giving interesting information on the GO modifications produced by the ionization effects due to the X-ray exposition. Despite the background fluctuations, the less intense C═C&C═O peak shows a transmittance which decreases with the oxidation process, both at 10 kV and at 30 kV in air, proportionally to the X-ray irradiation time. Instead, in vacuum this transmittance increases, or remains almost constant, as result of a significant GO reduction due to the decrement of carbonyl C═O bonds, as shown in the plot of Fig. 9b.

In both cases plotted in Fig. 9 the X-ray irradiation in air is referred to the use of the 3 cm distance from the X-ray tube collimator.

Finally, an interesting result is obtained observing the FTIR peak transmittance due to the presence of CO_2 molecules around 2365 cm^{-1}. Although the CO_2 transmission peak has low intensity, it is worth to be mentioned. In fact, measurements show that the CO_2 peak grows with the X-ray exposition time for irradiations both in air and vacuum. This means that its formation is not due to the presence of gas externally to the GO foil, like air, but it is generated by the C–O or O–H bonds breaking resulting in the C and O free radicals formation and their subsequent atomic reaction. In order to better observe the CO_2 generation versus the X-ray irradiation time for air and vacuum exposition, the net peak transmittance intensity has been calculated subtracting the background from the peak at 2365 cm^{-1}. The obtained results, in terms of relative transmittance variation versus the irradiation time for the different cases, are shown in the plot of Fig. 10. The fact that the CO_2 molecules are generated not only in air but also in vacuum, confirms the above suggested hypothesis according to which they are produced into the X-ray irradiated GO material as result of the chemical reactions

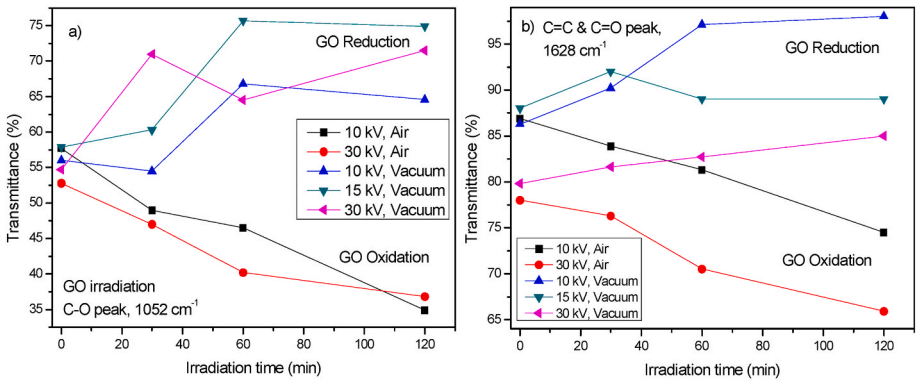

Fig. 9. FTIR C–O (a) and C═C&C═O (b) peak transmittance versus the X-ray irradiation time for air and vacuum irradiations and for different X-ray tube bias voltages.

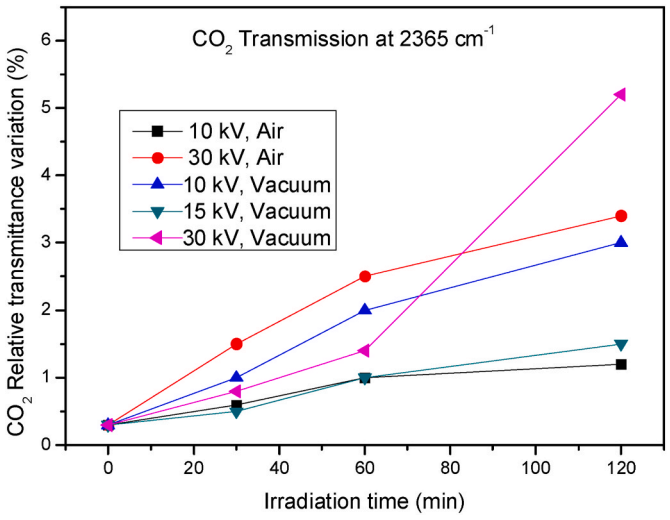

Fig. 10. CO_2 relative transmittance variation versus the X-ray irradiation time for air and vacuum irradiations at different X-ray tube bias voltages.

between carbon and oxygen free radicals developed by the X-ray energy deposition which, in this case, promotes a chemical reaction between the desorbed species coming from the GO matrix.

4. Conclusions and final remarks

Graphene oxidation could be enhanced irradiating GO with ionizing radiation in air or in gases containing oxygen, obtaining high insulating interlamellar materials rich with functional oxygen groups. In vacuum or inert gases the ionizing radiations reduce the oxygen content in GO, obtaining interlamellar conductive rGO with properties more and more similar to that of graphene with increasing of the absorbed dose.

Graphene oxide foils have been exposed to X-rays irradiations in air and in vacuum by varying the bias voltage applied to the X-ray tube and the exposure time. Although different analysis techniques could be adopted to measure the enhancement or reduction of oxidation, the GO modifications have been analyzed using the simple but highly accurate attenuated total reflectance method coupled to Fourier Transmission Infrared (ATR-FTIR) spectroscopy.

The X-rays irradiation in air produces an increment of the pristine GO oxidation as a consequence of the ionization and chemical bond breaking with an increment of the oxygen functional groups, water and CO_2 content attributable to the oxygen of the air. The observed oxidation process increases with the irradiation time showing a little saturation at high X-ray exposure times. The dependence on the X-ray energy in the X-ray tube (10–30) kV voltage range slightly affects the oxidation, even if a minor effect is observed at the highest energies due to the lowest absorbance of the material.

On the contrary, the reported results have indicated that the X-ray irradiation in vacuum produces a reduction of the pristine GO due to the ionization and chemical bonds breaking with a significant decrement of the oxygen functional groups, water and CO_2 content, which is assisted by their significant desorption for the action of the vacuum system pumping. The reduction process grows up with the X-ray irradiation time showing a little saturation at high time values. The dependence on the X-ray energy in the X-ray tube (10–30) kV voltage range has little influence on the GO reduction, even if a less significant effect is observed at the highest energies due to the lowest absorbance of the material.

The effects of GO oxidation in air and of GO reduction in vacuum under X-ray irradiation confirm our similar results obtained using IR laser [19,38] and can be applied to the devices based on GO and rGO which work under the action of ionizing radiations, such as soft X-rays. The GO oxidation gives rise to a material more insulating from the point of view of electrical and thermal conductivity, more absorbent to IR radiations for the presence of the oxygen functional groups, hydrophilic, light, and rich in water. Instead, the GO reduction gives rise to a material conductive from the point of electrical and thermal properties, more transparent to IR radiations, hydrophobic and more dense, due to the decrement of the oxygen functional groups and water, depending on its reduction level.

The observed effects of GO exposure to X-rays with bias voltages ranging from 10 kV to 30 kV can be employed to build biocompatible and water equivalent dosimeters and foil detectors for X-ray beams. Of course, these effects are maintained if the foil is preserved in vacuum or in inert environment and not in air. Moreover, the GO modifications change its structure and composition and consequently its physical and chemical properties. For example, they may change the diffusion coefficients of gases in GO membranes which undergo strong changes going from the highly oxidized, low density GO, to the reduced, high density and more compact GO, according to the literature data [17].

Further investigations on the GO modifications under X-ray irradiation are in progress to evaluate their dependence on a larger X-ray energy range, on the absorbed dose and absorbed dose-rate in different, inert or reactive, environments.

CRediT authorship contribution statement

L. Torrisi: Writing – original draft, Supervision, Funding acquisition, Conceptualization. **M. Cutroneo:** Investigation, Funding acquisition, Data curation. **A. Torrisi:** Writing – review & editing, Resources, Investigation. **L. Silipigni:** Writing – review & editing, Investigation.

Declaration of competing interest

Author declare to have no conflict of interest for this article.

Data availability

Data will be made available on request.

Acknowledgments

Authors thank INFN for the financial support given to the CIMA experiment developed at the Catania Section, Italy, under the coordination of Prof. L. Torrisi. This publication was supported by OP RDE, MEYS, Czech Republic under the project CANAM OP, CZ.02.1.01/0.0/0.0/16_013/0001812 and by the Czech Science Foundation (GACR No. 23-06702S).

References

[1] V. Skakalova, A. Kaiser (Eds.), Graphene, Properties, Preparation, Characterization and Applications, second ed. –, Elsevier, Amsterdam, 2021. June 23.
[2] M. Aliofkhazraei, N. Ali, W.I. Milne, C.S. Ozkan, S. Mitura, J.L. Gervasoni, Electrical and Optical Properties, CRC Press Taylor & Francis group, Boca Raton, 2016.
[3] X. Chen, Z. Qu, Z. Liu, G. Ren, Mechanism of oxidization of graphite to graphene oxide by the hummers method, ACS Omega 7 (2022) 23503–23510, 27.
[4] L. Torrisi, M. Cutroneo, V. Havranek, L. Silipigni, B. Fazio, M. Fazio, G. Di Marco, A. Stassi, A. Torrisi, Self-supporting graphene oxide films preparation and characterization methods, Vacuum 160 (2019) 1–11.
[5] R. Zulkharnay, O. Ualibek, O. Toktarbaiuly, P.W. May, Hydrophobic behaviour of reduced graphene oxide thin film fabricated via electrostatic spray deposition, Bull. Mater. Sci. 44 (2021) 112.
[6] M. Aliofkhazraei, N. Ali, W.I. Milne, C.S. Ozkan, S. Mitura, J.L. Gervasoni, Mechanical and Chemical Properties, CRC Press Taylor & Francis group, Boca Raton, 2016.
[7] L. Torrisi, L. Silipigni, D. Manno, A. Serra, V. Nassisi, M. Cutroneo, A. Torrisi, Investigations on graphene oxide for ion beam dosimetry applications, Vacuum 178 (2020), 109451.
[8] W.H. Zhang, M.J. Yin, Q. Zhao, C.G. Jin, N. Wang, S. Ji, C.L. Ritt, M. Elimelech, Q. F. An, Graphene oxide membranes with stable porous structure for ultrafast water transport, Nat. Nanotechnol. 16 (2021) 337–343.

[9] L. Silipigni, G. Salvato, B. Fazio, G. Di Marco, E. Proverbio, M. Cutroneo, A. Torrisi, L. Torrisi, Temperature sensor based on IR-laser reduced Graphene Oxide, J. Inst. Met. 15 (1) (2020) 1–11. C04006.
[10] L. Torrisi, V. Havranek, A. Torrisi, M. Cutroneo, L. Silipigni, Laser and ion beams graphene oxide reduction for microelectronic devices, Radiat. Eff. Defect Solid 175 (3–4) (2020) 226–240.
[11] J. Wu, H. Lin, D.J. Moss, K.P. Loh, B. Jia, Graphene oxide for photonics, electronics and optoelectronics, Nat. Rev. Chem (2023), https://doi.org/10.1038/s41570-022-00458-7.
[12] L. Torrisi, L. Silipigni, G. Salvato, Graphene oxide/Cu junction as relative humidity sensor, J. Mater. Sci. Mater. Electron. 31 (14) (2020) 11001–11009.
[13] D.H. Tien, J.Y. Park, K.B. Kim, N. Lee, Y. Seo, Characterization of graphene-based FET fabricated using a shadow mask, Sci. Rep. 6 (25050) (2016) 1–8.
[14] F.T. Johra, J.W. Lee, W.G. Jung, Facile and safe graphene preparation on solution based platform, J. Ind. Eng. Chem. 20 (2014) 2883–2887.
[15] R. Al-Gaashani, A. Najjar, Y. Zakaria, S. Mansour, M.A. Atieh, XPS and structural studies of high quality graphene oxide and reduced graphene oxide prepared by different chemical oxidation methods, Ceram. Int. 45 (11) (2019) 14439–14448.
[16] L. Torrisi, G. Salvato, M. Cutroneo, F. Librizzi, A. Torrisi, L. Silipigni, Source-drain electrical conduction and radiation detection in graphene-based field effect transistor (GFET), J. Inst. Met. 17 (2022) 1–13. P02008.
[17] M. Cutroneo, V. Havranek, A. Mackova, V. Semian, L. Torrisi, L. Calcagno, Micro-patterns fabrication using focused proton beam lithography, Nucl. Instrum. Methods B 371 (2016) 344–349.
[18] L. Silipigni, M. Fazio, B. Fazio, M. Cutroneo, L. Torrisi, Tailoring the oxygen content of graphene oxide by IR laser irradiation, Appl. Phys. A 124 (2018) 1–12, 545.
[19] L. Torrisi, L. Silipigni, M. Cutroneo, Radiation effects of IR laser on graphene oxide irradiated in vacuum and in air, Vacuum 153 (2018) 122–131.
[20] L. Torrisi, M. Cutroneo, A. Torrisi, L. Silipigni, Measurements on five characterizing properties of graphene oxide and reduced graphene oxide foils, Phys. Solid State (2022) 1–9, 2100628.
[21] M. Cutroneo, V. Havranek, A. Mackova, P. Malinsky, L. Torrisi, L. Silipigni, B. Fazio, A. Torrisi, K. Szokolova, Z. Sofer, J. Stammers, Effects of the ion bombardment on the structure and composition of GO and rGO foils, Mater. Chem. Phys. 232 (2019) 272–277.
[22] D. Manno, A. Serra, A. Buccolieri, L. Calcagnile, M. Cutroneo, A. Torrisi, L. Silipigni, L. Torrisi, Structural and spectroscopic investigations on graphene oxide foils irradiated by ion beams for dosimetry application, Vacuum 188 (2021), 110185.
[23] L. Torrisi, M. Cutroneo, A. Torrisi, L. Silipigni, Nitrogen diffusion in graphene oxide and reduced graphene oxide foils, Vacuum 194 (2021), 110632.
[24] M. Ye, J. Gao, Y. Xiao, T. Xu, Y. Zhao, L. Qu, Metal/graphene oxide batteries, Carbon 125 (2017) 299–307.
[25] H. Seo, S. Ahn, J. Kim, Y.A. Lee, K.H. Chung, K.-J. Jeon, Multi-resistive reduced graphene oxide diode with reversible surface electrochemical reaction induced carrier control, Sci. Rep. 4 (2014) 5642.
[26] L. Torrisi, V. Havranek, M. Cutroneo, A. Mackova, L. Silipigni, A. Torrisi, Characterization of reduced Graphene oxide films used as stripper foils in a 3.0-MV Tandetron, Radiat. Phys. Chem. 165 (2019), 108397.
[27] L. Torrisi, M. Cutroneo, A. Torrisi, Protons and carbon ions acceleration in the target-normal-sheath-acceleration regime using low-contrast fs laser and metal-graphene targets, Contrib. Plasma Phys. 60 (1) (2019), e201900076.
[28] D. Kornilov, T.R. Penki, A. Cheglakov, D. Aurbach, Li/graphene oxide primary battery system and mechanism, Battery Energy 1 (2) (2022), 20210002.
[29] L. Torrisi, V. Havranek, L. Silipigni, A. Torrisi, M. Cutroneo, Conductive tracks in graphene oxide foils induced by micro beams of MeV helium ions, Diam. Relat. Mater. 128 (2022), 109281.
[30] Y.S. Chang, F.K. Chen, D.C. Tsai, B.H. Kuo, F.S. Shieu, N-doped reduced graphene oxide for room-temperature NO gas sensors, Scientifc Reports 11 (2021), 20719.
[31] L. Torrisi, L. Silipigni, M. Cutroneo, E. Proverbio, A. Torrisi, Linear Energy Transfer (LET) dependence of graphene oxide dosimeter for different ionizing radiations, Vacuum 203 (2022), 111240.
[32] L. Torrisi, L. Silipigni, M. Cutroneo, A. Torrisi, Graphene oxide as a radiation sensitive material for XPS dosimetry, Vacuum 173 (2020) 1–8, 109175.
[33] Graphenea, High Quality Graphene Producer, Actual Website 2023: High Quality Graphene Producer – Graphenea EU.
[34] Ametek, Mini-X2 X-Ray Tube, Actual Website 2023: Mini-X2 X-Ray Tube System for XRF – Amptek – X-Ray Detectors and Electronics.
[35] Jasco, FTIR 5600 Spectrometer, Actual Website 2023: JASCO Asia Portal - FT/IR-4600 FT-IR Spectrometer - (jascoint.co.jp).
[36] A. Alizadeh, G. Abdi, M.M. Khodaei, M. Ashokkumar, J. Amirian, Graphene oxide/Fe3O4/SO3H nanohybrid: a new adsorbent for adsorption and reduction of Cr(VI) from aqueous solutions, RSC Adv. 7 (2017) 14876–14887.
[37] Sudesh, N. Kumar, S. Das, C. Bernhard, G.D. Varma, Effect of graphene oxide doping on superconducting properties of bulk MgB2, Supercond. Sci. Technol. 26 (2013), 095008.
[38] L. Torrisi, M. Cutroneo, L. Silipigni, M. Fazio, A. Torrisi, Effects of the laser irradiation on graphene oxide foils in vacuum and air, Phys. Solid State 61 (7) (2019) 1327–1331.